THE EUROPEAN
PHYSICAL JOURNAL C

Model independent analysis of $B^* \to P\ell\bar{\nu}_\ell$ decay processes

Atasi Ray[1,a], Suchismita Sahoo[2,b], Rukmani Mohanta[1,c]

[1] School of Physics, University of Hyderabad, Hyderabad 500046, India
[2] Theoretical Physics Division, Physical Research Laboratory, Ahmedabad 380009, India

Abstract Very compelling deviations in the recently observed lepton nonuniversality observables $(R_{D^{(*)}}, R_{K^{(*)}}, R_{J/\psi})$ of semileptonic B meson decays from their Standard Model predictions hint towards the presence of some kind of new physics beyond it. In this regard, we investigate the effect of new physics in the semileptonic $\bar{B}^*_{d(s)} \to P\ell\bar{\nu}_\ell$ decay processes, where $P = D, \pi(D_s, K)$, in a model independent way. We consider the presence of additional vector and scalar type interactions and constrain the corresponding new couplings by fitting $\mathrm{Br}(B_u^+ \to \tau^+\nu_\tau)$, $\mathrm{Br}(B \to \pi\tau\bar{\nu}_\tau)$, $\mathrm{Br}(B_c^+ \to \tau^+\nu_\tau)$, R_π^l, $R_{D^{(*)}}$ and $R_{J/\psi}$ data. Using the constrained new parameters, we estimate the branching ratios, forward–backward asymmetry, lepton-spin asymmetry and lepton non-universality observables of $\bar{B}^*_{d,s} \to P\tau\bar{\nu}_\tau$ processes. We find that the branching ratios of these decay modes are sizeable and deviate significantly (for vector-type couplings) from their corresponding standard model values, which are expected to be within the reach of Run III of Large Hadron Collider experiment.

1 Introduction

In the last few years, several intriguing hints of new physics (NP) have been observed in the form of lepton flavour universality violating (LFUV) observables in semileptonic B decays. In particular, the observables $R_{D^{(*)}} = \mathrm{Br}(B \to D^{(*)}\tau\bar{\nu}_\tau)/\mathrm{Br}(B \to D^{(*)}l\bar{\nu}_l)$, with $l = e, \mu$ in the charged-current transition $b \to c\ell\bar{\nu}_\ell$, measured by BaBar [1,2] Belle [3–6] and LHCb [7–9] Collaborations, with the following avarage values as determined by Heavy Flavour Averaging Group (HFLAV) [10]

$$R_D = 0.340 \pm 0.027 \pm 0.013,$$
$$R_{D^*} = 0.295 \pm 0.011 \pm 0.008, \tag{1}$$

[a] e-mail: atasiray92@gmail.com
[b] e-mail: suchismita8792@gmail.com
[c] e-mail: rmsp@uohyd.ac.in

with $R_D - R_{D^*}$ correlation of -0.38, indicate $\sim 3.08\sigma$ discrepancy with their corresponding Standard Model (SM) predictions

$$R_D^{\mathrm{SM}} = 0.299 \pm 0.003, \quad R_{D^*}^{\mathrm{SM}} = 0.258 \pm 0.005. \tag{2}$$

The recently measured $R_{J/\psi} = \mathrm{Br}(B_c \to J/\psi\tau\bar{\nu}_\tau)/\mathrm{Br}(B_c \to J/\psi l\bar{\nu}_l) = 0.71 \pm 0.17 \pm 0.184$ parameter by LHCb Collaboration [11] is in the same line and has nearly 2σ deviation from its SM value $R_{J/\psi} = 0.289 \pm 0.01$ [12,13]. Similarly, in the semileptonic $B \to K^{(*)}\ell\ell$ decay processes, mediated by the neutral current transition $b \to s\ell\ell$, 2.6σ and $(2.2-2.4)\sigma$ deviations have been observed in the measured values of $R_K = \mathrm{Br}(B^+ \to K^+\mu^+\mu^-)/\mathrm{Br}(B^+ \to K^+e^+e^-)$ [14] and $R_{K^*} = \mathrm{Br}(\bar{B}^0 \to \bar{K}^*\mu^+\mu^-)/\mathrm{Br}(\bar{B}^0 \to \bar{K}^*e^+e^-)$ [15] with values

$$R_K|_{q^2\in[1,6]\,\mathrm{GeV}^2} = 0.745^{+0.090}_{-0.074} \pm 0.036,$$
$$R_{K^*}|_{q^2\in[0.045,1.1]\,\mathrm{GeV}^2} = 0.66^{+0.11}_{-0.07} \pm 0.03,$$
$$R_{K^*}|_{q^2\in[1.1,6]\,\mathrm{GeV}^2} = 0.69^{+0.11}_{-0.07} \pm 0.05, \tag{3}$$

from their corresponding SM predictions [16,17]

$$R_K^{\mathrm{SM}}|_{q^2\in[1,6]\,\mathrm{GeV}^2} = 1.003 \pm 0.0001,$$
$$R_{K^*}\mathrm{SM}|_{q^2\in[0.045,1.1]\,\mathrm{GeV}^2} = 0.92 \pm 0.02,$$
$$R_{K^*}^{\mathrm{SM}}|_{q^2\in[1.1,6]\,\mathrm{GeV}^2} = 1.00 \pm 0.01. \tag{4}$$

Recently, the LHCb experiment has announced its updated measurements on R_K [18] and the Belle Collaboration has announced new R_{K^*} [19] results. After combining the Run 1 and Run 2 data, though the updated experimental value of $R_K = 0.846^{+0.060}_{-0.054}(\mathrm{stat})^{+0.016}_{-0.014}(\mathrm{syst})$ [18] is closer to the SM prediction, the discrepancy still persists at the level of $\sim 2.5\sigma$, due to the reduced errors. The errors in the new measurements on $R_{K^*} = 0.52^{+0.36}_{-0.26} \pm 0.005$ $(0.96^{+0.45}_{-0.29} \pm 0.11)$ observable in the $q^2 \in [0.045, 1.1]\,\mathrm{GeV}^2$ $(q^2 \in [1.1, 6]\,\mathrm{GeV}^2)$ bin, reported by the Belle Collaboration [19] are quite a bit larger than the errors in the previous LHCb masurement. Additionally, a small discrepancy has also been

reported in the $b \to u\ell\bar{\nu}$ mediated process defined as $R_\pi^l = \frac{\tau_{B0}}{\tau_{B^-}}(\mathrm{Br}(B^- \to \tau^-\bar{\nu}_\tau)/\mathrm{Br}(B^0 \to \pi^+ l^-\bar{\nu}_l))$ [20]. As all these observables are ratios of branching fractions, the theoretical uncertainties due to the CKM matrix elements and hadronic form factors cancel out to a large extent, resulting the prediction with high accuracy. Therefore, the lepton flavor universality violating tests are considered to be the most powerful tools to probe new physics beyond the standard model. Tremendous effort has been made in the last few years to understand the nature of NP, which might be responsible for such deviations.

Being motivated by these observed anomalies in various B meson decays, in this work we would like to investigate the impact of new physics on the differential decay rate and various other observables like forward–backward asymmetry, lepton-spin asymmetry and lepton nonuniversality (LNU) observable of weakly decaying vector $B_{d,(s)}^*$ meson to a pseudoscalar $P(= D(D_s), \pi(K))$ meson mediated through the quark level transitions $b \to (c,u)\ell\bar{\nu}_\ell$. Although such hadrons decay primarily through the electromagnetic process $B_{d,s}^* \to B_{d,s}\gamma$, and their weak decay channels are expected to be quite suppressed, the situation has improved considerably with the advent of the high luminosity Belle II experiment. For instance, as discussed in Ref. [21], using the production cross section of $\Upsilon(5S)$ in e^-e^+ collision as $\sigma(e^+e^- \to \Upsilon(5S)) = 0.301$nb and $\mathrm{Br}(\Upsilon(5S) \to B^*\bar{B}^*) = (38.1 \pm 3.4)\%$ [20], about 4×10^9 B^* meson pairs $(B_{u,d}^* + \bar{B}_{u,d}^*)$ are expected to be produced per year. This in turn implies that the rare B^* decay modes with branching fraction $> \mathcal{O}(10^{-9})$ are likely to be observed at Belle II. Hence, Belle II experiment would be quite instrumental in search for the rare decay modes of the excited B mesons. In addition the LHC experiment will also play a pivotal role in the search for B^* decay channels, as the production cross section of $\Upsilon(5S)$ is much larger in $p\bar{p}$ collision compared to e^+e^- collision. On the other hand, the study of B^* meson decays has also received considerable attention in recent times. In the literature [22–25], the leptonic decay modes of $B_{s,d}^*$ mesons are investigated in SM and in the context of various new physics models. The analysis of semileptonic weak decays $B^* \to P\ell\nu$ both in the SM and in the presence of NP are discussed in the Refs. [21,26,27].

The layout of the paper is as follows. In Sect. 2, we illustrate the theoretical framework required to analyse the decay processes $B^* \to P\ell\nu$ in the effective theory formalism. The expressions for the differential decay rate and other observables like forward–backward asymmetry, lepton nonuniversality (R_P^*) and the lepton-spin asymmetry are presented in this section. The constraints on the new couplings using χ^2 fit from $R_{D^{(*)}}$, $R_{J/\psi}$, R_π^l, $\mathrm{Br}(B_{u,c} \to \tau\nu)$, $\mathrm{Br}(B \to \pi\tau\bar{\nu})$ observables are obtained in Sect. 3. Our results are discussed in Sect. 4 followed by the summary of our work in Sect. 5.

2 Theoretical framework

The most general effective Lagrangian for $B^* \to P\ell\bar{\nu}_\ell$ processes mediated by $b \to q\ell^-\bar{\nu}_\ell$ ($q = u, c$), in the effective field theory approach can be expressed as [28],

$$\mathcal{L}_{eff} = -2\sqrt{2}G_F V_{qb}[(1 + V_L)\,\bar{q}_L\gamma^\mu b_L\,\bar{\ell}_L\gamma_\mu \nu_L$$
$$+ V_R\,\bar{q}_R\gamma^\mu b_R\,\bar{\ell}_L\gamma_\mu \nu_L + S_L\,\bar{q}_R b_L\,\bar{\ell}_R \nu_L$$
$$+ S_R\,\bar{q}_L b_R\,\bar{\ell}_R \nu_L + T_L\,\bar{q}_R\sigma^{\mu\nu}b_L\,\bar{\ell}_R\sigma_{\mu\nu}\nu_L + \text{h.c.}],$$
$$(5)$$

where P is any pseudoscalar meson, G_F is the Fermi constant, V_{qb} is the CKM matrix element, $V_{L,R}$, $S_{L,R}$, T_L are the new vector, scalar, and tensor type new physics couplings, which are zero in the standard model. All these new physics couplings are considered to be complex. Furthermore, we consider the neutrinos as left handed. We assume the NP effect is mainly through the third generation leptons and do not consider the effect of tensor operators in our analysis for simplicity. Here $(q, \ell)_{L,R} = P_{L,R}(q, \ell)$, where $P_{L,R} = (1 \mp \gamma_5)/2$ are the chiral projection operators.

We consider the kinematics of the decay process $B^* \to P\ell\bar{\nu}_\ell$ using helicity amplitudes. In this formalism, the decay process $B^* \to P\ell\bar{\nu}_\ell$ is considered to proceed through $\bar{B}^* \to PW^{*-}$, where the off-shell W^{*-} decays to $\ell^-\bar{\nu}_\ell$. One can write the amplitude from Eq. (5) as

$$\mathcal{M}(B^* \to P\ell\bar{\nu}_\ell)$$
$$= \frac{G_F}{\sqrt{2}}V_{qb}\sum_k C_k(\mu)\langle P|\bar{q}\Gamma^k b|B^*\rangle\,\bar{u}_\ell\Gamma_k v_\nu, \quad (6)$$

where $C_k(\mu)$ represents the Wilson coefficient with values

$$C_k(\mu) = \begin{cases} 1 & \text{for SM,} \\ V_{L,R}, S_{L,R} & \text{for NP beyond SM,} \end{cases}$$

Γ^k denotes the product of gamma matrices, which gives rise to different Lorentz structure of hadronic and leptonic currents of Eq. (5) i.e., $\Gamma^k = \gamma^\mu(1\pm\gamma_5)$, and $(1\pm\gamma_5)$. Hence, the square of the matrix element can be expressed as the product of leptonic ($L_{\mu\nu}$) and hadronic ($H^{\mu\nu}$) tensors (related to the corresponding helicity amplitudes)

$$\left|\mathcal{M}(B^* \to P\ell\bar{\nu}_\ell)\right|^2 = \frac{G_F^2}{2}|V_{qb}|^2\sum_{i,j}C_{ij}(\mu)(L_{\mu\nu}^{ij}H^{\mu\nu,ij}),$$
$$(7)$$

where the superscripts i, j represent the combination of four operators $(V \mp A)$, $(S \mp P)$ in the effective Lagrangian (5), $C_{ij}(\mu)$ denotes the product of Wilson coefficients C_i and C_j. We omit these superscripts in the following discussion for convenience. It should be noted that, the polarization vector of the off-shell particle W^* ($\bar{\epsilon}^\mu(m)$), satisfies the following orthonormality and completeness relations:

$$\bar{\epsilon}^{*\mu}(m)\bar{\epsilon}_\mu(m') = g_{mm'},$$

$$\sum_{mm'} \bar{\epsilon}^{*\mu}(m)\bar{\epsilon}^\nu(m')g_{mm'} = g^{\mu\nu}, \tag{8}$$

where $g_{mm'} = \text{diag}(+, -, -, -)$ and $m, m' = \pm, 0, t$ represent the transverse, longitudinal and time-like polarization components. Now inserting the completeness relation from Eq. (8) into (7), the product of $L_{\mu\nu}$ and $H^{\mu\nu}$ can be expressed as

$$L_{\mu\nu}H^{\mu\nu} = \sum_{m,m',n,n'} L(m,n)H(m',n')g_{mm'}g_{nn'}, \tag{9}$$

where $L(m,n) = L^{\mu\nu}\bar{\epsilon}_\mu(m)\bar{\epsilon}_\nu^*(n)$ and $H(m,n) = H^{\mu\nu}\bar{\epsilon}_\mu^*(m)\bar{\epsilon}_\nu(n)$ are the Lorentz invariant parameters, and hence their values are independent of any specific reference frame. So for calculational convenience, we will evaluate $H(m,n)$ in the B^* rest frame and $L(m,n)$ in $\ell - \bar{\nu}_\ell$ center of mass frame as discussed in [21,26].

2.1 Hadronic helicity amplitudes

In the rest frame of B^* meson, we consider the pseudoscalar meson P to be moving along the positive z-direction. The polarization vector of the virtual W^* boson are chosen to be

$$\bar{\epsilon}^\mu(t) = \frac{1}{q^2}(q_0, 0, 0, -|\vec{p}|), \quad \bar{\epsilon}^\mu(0) = \frac{1}{q^2}(|\vec{p}|, 0, 0, -q_0),$$

$$\bar{\epsilon}^\mu(\pm) = \frac{1}{\sqrt{2}}(0, \pm 1, -i, 0), \tag{10}$$

where $q_0 = (m_{B^*}^2 - m_P^2 + q^2)/2m_{B^*}$, $|\vec{p}| = \lambda^{1/2}(m_{B^*}^2, m_P^2, q^2)/2m_B^*$, $q^2 = (p_{B^*} - p_P)^2$, is the momentum transferred square and $\lambda(a, b, c) = a^2 + b^2 + c^2 - 2(ab + bc + ca)$. The polarization vector of the on-shell B^* meson $\varepsilon^\mu(m = 0, \pm)$, takes the form

$$\varepsilon^\mu(0) = (0, 0, 0, 1), \quad \varepsilon^\mu(\pm) = \frac{1}{\sqrt{2}}(0, \mp 1, -i, 0). \tag{11}$$

In order to calculate the hadronic helicity amplitudes, we use the following matrix elements of $B^* \to P$ transition

$$\langle P(p_P)|\bar{q}\gamma_\mu b|\bar{B}^*(\varepsilon, p_{B^*})\rangle$$

$$= -\frac{2iV(q^2)}{m_{B^*} + m_P}\epsilon_{\mu\nu\rho\sigma}\varepsilon^\nu p_P^\rho p_{B^*}^\sigma,$$

$$\langle P(p_P)|\bar{q}\gamma_\mu\gamma_5 b|\bar{B}^*(\varepsilon, p_{B^*})\rangle = 2m_{B^*}A_0(q^2)\frac{\varepsilon \cdot q}{q^2}q_\mu$$

$$+ (m_P + m_{B^*})A_1(q^2)\left(\varepsilon_\mu - \frac{\varepsilon \cdot q}{q^2}q_\mu\right)$$

$$+ A_2(q^2)\frac{\varepsilon \cdot q}{m_P + m_{B^*}}\left[(p_{B^*} + p_P)_\mu - \frac{m_{B^*}^2 - m_P^2}{q^2}q_\mu\right], \tag{12}$$

where $V(q^2)$, $A_{0,1,2}(q^2)$ are the various form factors. The matrix elements for the scalar and pseudoscalar currents can be obtained by using the equation of motion

$$i\partial_\mu(\bar{q}\gamma^\mu b) = (m_b - m_q)\bar{q}b,$$

$$i\partial_\mu(\bar{q}\gamma^\mu\gamma_5 b) = -(m_b + m_q)\bar{q}\gamma_5 b, \tag{13}$$

as

$$\langle P(p_P)|\bar{q}b|\bar{B}^*(\varepsilon, p_{B^*})\rangle = 0,$$

$$\langle P(p_P)|\bar{q}\gamma_5 b|\bar{B}^*(\varepsilon, p_{B^*})\rangle = -(\varepsilon \cdot q)\frac{2m_{B^*}}{m_b + m_q}A_0(q^2), \tag{14}$$

where the $m_{b,q}$ represent the current quark masses evaluated at the b-quark mass scale. The helicity amplitudes are defined as

$$H_{\lambda_{B^*}\lambda_{W^*}}^{V_L}(q^2) = \bar{\epsilon}^{*\mu}(\lambda_{W^*})\langle P(p_P)|\bar{q}\gamma_\mu(1 - \gamma_5)b|\bar{B}^*(\varepsilon(\lambda_{B^*}), p_{B^*})\rangle,$$

$$H_{\lambda_{B^*}\lambda_{W^*}}^{V_R}(q^2) = \bar{\epsilon}^{*\mu}(\lambda_{W^*})\langle P(p_P)|\bar{q}\gamma_\mu(1 + \gamma_5)b|\bar{B}^*(\varepsilon(\lambda_{B^*}), p_{B^*})\rangle,$$

$$H_{\lambda_{B^*}\lambda_{W^*}}^{S_L}(q^2) = \langle P(p_P)|\bar{q}(1 - \gamma_5)b|\bar{B}^*(\varepsilon(\lambda_{B^*}), p_{B^*})\rangle,$$

$$H_{\lambda_{B^*}\lambda_{W^*}}^{S_R}(q^2) = \langle P(p_P)|\bar{q}(1 + \gamma_5)b|\bar{B}^*(\varepsilon(\lambda_{B^*}), p_{B^*})\rangle, \tag{15}$$

where for convenience, we use the notations $\lambda_{B^*} = 0, \pm$ and $\lambda_{W^*} = 0, \pm, t$ to represent the helicity states of the B^* and W^* boson. Thus, with Eqs. (12), (14) and (15), one obtains the following non-vanishing helicity amplitudes

$$H_{0t}(q^2) = H_{0t}^{V_L}(q^2) = -H_{0t}^{V_R}(q^2) = \frac{2m_{B^*}|\vec{p}|}{\sqrt{q^2}}A_0(q^2),$$

$$H_{00}(q^2) = H_{00}^{V_L}(q^2) = -H_{00}^{V_R}(q^2)$$

$$= \frac{1}{2m_{B^*}\sqrt{q^2}}\left[(m_{B^*} + m_P)(m_{B^*}^2 - m_P^2 + q^2)A_1(q^2) + \frac{4m_{B^*}^2|\vec{p}|^2}{m_{B^*} + m_P}A_2(q^2)\right],$$

$$H_{\pm\mp}(q^2) = H_{\pm\mp}^{V_L}(q^2) = -H_{\mp\pm}^{V_R}(q^2)$$

$$= -(m_{B^*} + m_P)A_1(q^2) \mp \frac{2m_{B^*}|\vec{p}|}{m_{B^*} + m_P}V(q^2),$$

$$H_{0t}' = H_{0t}^{S_L}(q^2) = -H_{0t}^{S_R}(q^2) = -\frac{2m_{B^*}|\vec{p}|}{m_b + m_q}A_0(q^2). \tag{16}$$

2.2 Leptonic helicity amplitudes

The leptonic helicity amplitudes are defined as

$$h_{\lambda_\ell,\lambda_{\bar{\nu}_\ell}}^i = \frac{1}{2}\bar{\epsilon}_\mu(\lambda_{W^*})\bar{u}_\ell(\lambda_\ell)\Gamma^i v_{\bar{\nu}_\ell}(\lambda_{\bar{\nu}_\ell}), \tag{17}$$

where $\lambda_{W^*} = \lambda_\ell - \lambda_{\bar{\nu}_\ell}$, $i = V_{L,R}, S_{L,R}$, and $\Gamma^{V_{L,R}} = \gamma^\mu(1 \mp \gamma_5)$, $\Gamma^{S_{L,R}} = (1 \mp \gamma_5)$. In the center of mass frame of $\ell - \bar{\nu}_\ell$, the four momenta of ℓ and $\bar{\nu}_\ell$ pair are expressed as

$$p_\ell^\mu = (E_\ell, |\vec{p}_\ell|\sin\theta, 0, |\vec{p}_\ell|\cos\theta),$$

$$p_{\nu_\ell}^\mu = (|\vec{p}_\ell|, -|\vec{p}_\ell|\sin\theta, 0, -|\vec{p}_\ell|\cos\theta), \tag{18}$$

where $E_\ell = (q^2 + m_\ell^2)/2\sqrt{q^2}$, $|\vec{p}_\ell| = (q^2 - m_\ell^2)/2\sqrt{q^2}$ and θ is the angle between the three momenta of of P and ℓ. The polarization vector of the virtual W^* boson in this frame is

$$\bar{\epsilon}^\mu(t) = (1, 0, 0, 0), \quad \bar{\epsilon}^\mu(0) = (0, 0, 0, 1),$$
$$\bar{\epsilon}^\mu(\pm) = \frac{1}{\sqrt{2}}(0, \mp 1, -i, 0). \tag{19}$$

Thus, with Eqs. (17) and (19), one obtains the following non-vanishing contributions

$$|h_{-\frac{1}{2},\frac{1}{2}}^{V_{L,R}}|^2 = 8(q^2 - m_\ell^2), \quad |h_{\frac{1}{2},\frac{1}{2}}^{V_{L,R}}|^2 = 8\frac{m_\ell^2}{2q^2}(q^2 - m_l^2),$$
$$|h_{\frac{1}{2},\frac{1}{2}}^{S_{L,R}}|^2 = 4(q^2 - m_\ell^2), \quad |h_{\frac{1}{2},\frac{1}{2}}^{V_{L,R}}| \times |h_{\frac{1}{2},\frac{1}{2}}^{S_{L,R}}|$$
$$= 8\frac{m_\ell}{2\sqrt{q^2}}(q^2 - m_\ell^2). \tag{20}$$

2.3 Decay distribution and other observables

The double differential decay rate of $B^* \to P\ell\bar{\nu}_\ell$ decay process can be expressed as

$$\frac{d^2\Gamma}{dq^2 d\cos\theta} = \frac{G_F^2}{192\pi^3}\frac{|\vec{p}|}{m_{B^*}^2}|V_{qb}|^2\left(1 - \frac{m_\ell^2}{q^2}\right)$$
$$\times |\mathcal{M}(\bar{B}^* \to P\ell\bar{\nu}_\ell)|^2. \tag{21}$$

Now, with Eqs. (16) and (20), one can obtain $L_{\mu\nu}H^{\mu\nu}$ in terms of Wigner d^J-functions as [26]

$$L_{\mu\nu}H^{\mu\nu}$$
$$= \frac{1}{8}\sum_{\lambda_\ell,\lambda_\nu,\lambda_{W^*},\lambda'_{W^*},J,J'}(-1)^{J+J'}h^i_{\lambda_\ell,\lambda_\nu}h^{j*}_{\lambda_\ell,\lambda_\nu}\delta_{\lambda_{B^*},-\lambda_{W^*}}\delta_{\lambda_{B^*},-\lambda'_{W^*}}$$
$$\tag{22}$$
$$\times d^J_{\lambda_{W^*},\lambda_{\ell-1/2}}d^{J'}_{\lambda'_{W^*},\lambda_{\ell-1/2}}H^i_{\lambda_{B^*}\lambda_{W^*}}H^{j*}_{\lambda_{B^*}\lambda'_{W^*}}, \tag{23}$$

where J and J' take the values 0 and 1 and the various helicity components run over their allowed values. Thus, one can obtain the differential decay rate to particular leptonic helicity state ($\lambda = \pm\frac{1}{2}$) as

$$\frac{d^2\Gamma\left(\lambda_\ell = -\frac{1}{2}\right)}{dq^2 d\cos\theta} = \frac{G_F^2}{768\pi^3}\frac{|\vec{p}|}{m_{B^*}^2}|V_{qb}|^2\, q^2\left(1 - \frac{m_\ell^2}{q^2}\right)^2$$
$$\times\{|1 + V_L|^2[(1 - \cos\theta)^2 H_{-+}^2 + (1 + \cos\theta)^2 H_{+-}^2$$
$$+ 2\sin^2\theta H_{00}^2] + |V_R|^2[(1 - \cos\theta)^2 H_{+-}^2$$
$$+ (1 + \cos\theta)^2 H_{-+}^2 + 2\sin^2\theta H_{00}^2]$$
$$- 4\mathcal{R}e[(1 + V_L)V_R^*][(1 + \cos\theta)^2 H_{+-}H_{-+}$$
$$+ \sin^2\theta H_{00}^2]\}, \tag{24}$$

$$\frac{d^2\Gamma\left(\lambda_\ell = \frac{1}{2}\right)}{dq^2 d\cos\theta} = \frac{G_F^2}{768\pi^3}\frac{|\vec{p}|}{m_{B^*}^2}|V_{qb}|^2\left(1 - \frac{m_\ell^2}{q^2}\right)^2 m_\ell^2$$
$$\times\left\{(|1 + V_L|^2 + |V_R|^2)[\sin^2\theta(H_{-+}^2 + H_{+-}^2)\right.$$

$$+ 2(H_{0t} - \cos\theta H_{00})^2] - 4\mathcal{R}e[(1 + V_L)V_R^*]$$
$$\times[\sin^2\theta H_{-+}H_{+-} + (H_{0t} - \cos\theta H_{00})^2]$$
$$+ 4\mathcal{R}e[(1 + V_L - V_R)(S_L^* - S_R^*)]\frac{\sqrt{q^2}}{m_\ell}$$
$$\times[H'_{0t}(H_{0t} - \cos\theta H_{00})]$$
$$+ 2|S_L - S_R|^2\frac{q^2}{m_\ell^2}H'^2_{0t}\right\}. \tag{25}$$

From Eqs. (24) and (25), one can obtain the differential decay rate as

$$\frac{d\Gamma}{dq^2} = \frac{G_F^2}{288\pi^3}\frac{|\vec{p}|}{m_{B^*}^2}|V_{qb}|^2\, q^2\left(1 - \frac{m_\ell^2}{q^2}\right)^2\left[(|1 + V_L|^2 + |V_R|^2)\right.$$
$$\times\left[(H_{-+}^2 + H_{+-}^2 + H_{00}^2)\left(1 + \frac{m_\ell^2}{2q^2}\right) + \frac{3m_\ell^2}{2q^2}H_{0t}^2\right]$$
$$- 2\mathcal{R}e[(1 + V_L)V_R^*]\left[(2H_{-+}H_{+-}\right.$$
$$+ H_{00}^2)\left(1 + \frac{m_\ell^2}{2q^2}\right) + \frac{3m_\ell^2}{2q^2}H_{0t}^2\right]$$
$$+ 3\frac{m_\ell}{\sqrt{q^2}}\mathcal{R}e[(1 + V_L - V_R)(S_L^* - S_R^*)]H'_{0t}H_{0t}$$
$$\left. + \frac{3}{2}|S_L - S_R|^2 H'^2_{0t}\right], \tag{26}$$

where the values of the helicity amplitudes are given in Eq. (16).

Apart from the differential decay rate, the other NP sensitive observables, considered here are

- Lepton nonuniversality observable:

$$R_P^*(q^2) = \frac{d\Gamma(B^* \to P\tau^-\bar{\nu}_\tau)/dq^2}{d\Gamma(B^* \to Pl^-\bar{\nu}_l)/dq^2}, \tag{27}$$

where l denotes the light leptons $l = e, \mu$.

- Forward–backward asymmetry:

$$A_{\text{FB}}^P(q^2) = \frac{\int_{-1}^0 d\cos\theta(d^2\Gamma/dq^2 d\cos\theta) - \int_0^1 d\cos\theta(d^2\Gamma/dq^2 d\cos\theta)}{\int_{-1}^0 d\cos\theta(d^2\Gamma/dq^2 d\cos\theta) + \int_0^1 d\cos\theta(d^2\Gamma/dq^2 d\cos\theta)}, \tag{28}$$

which can be expressed in terms of the helicity amplitudes as

$$A_{\text{FB}}^P(q^2) = \frac{3}{4}\frac{X}{Y}, \tag{29}$$

where the parameters X and Y are given as

$$X = (|1 + V_L|^2 - |V_R|^2)(H_{-+}^2 - H_{+-}^2)$$
$$+ 2\left(\frac{m_\ell^2}{q^2}\right)(|1 + V_L|^2 + |V_R|^2)H_{0t}H_{00}$$

$$+4\mathcal{R}e[(1+V_L)V_R^*]\left(H_{+-}H_{-+}-\frac{m_\ell^2}{q^2}H_{0t}H_{00}\right)$$

$$+2\mathcal{R}e[(1+V_L-V_R)(S_L^*-S_R^*)]\frac{m_\ell}{\sqrt{q^2}}H_{0t}'H_{00},$$

$$Y=\left(|1+V_L|^2+|V_R|^2\right)\left[\left(H_{-+}^2+H_{+-}^2+H_{00}^2\right)\right.$$

$$\times\left(1+\frac{m_\ell^2}{2q^2}\right)+\frac{3m_\ell^2}{2q^2}H_{0t}^2\right]$$

$$-2\mathcal{R}e[(1+V_L)V_R^*]\left[(2H_{-+}H_{+-}+H_{00}^2)\right.$$

$$\times\left(1+\frac{m_\ell^2}{2q^2}\right)+\frac{3m_\ell^2}{2q^2}H_{0t}^2\right]$$

$$+3\frac{m_\ell}{\sqrt{q^2}}\mathcal{R}e[(1+V_L-V_R)(S_L^*-S_R^*)]H_{0t}'H_{0t}$$

$$+\frac{3}{2}|S_L-S_R|^2H_{0t}'^2. \tag{30}$$

- Lepton-spin asymmetry:

$$A_\lambda^P(q^2)=\frac{d\Gamma(\lambda_\ell=-1/2)/dq^2-d\Gamma(\lambda_\ell=1/2)/dq^2}{d\Gamma(\lambda_\ell=-1/2)/dq^2+d\Gamma(\lambda_\ell=1/2)/dq^2}. \tag{31}$$

2.4 Form factors and their q^2 dependence

The main inputs required for the numerical analysis are the values of the form factors. As the first principle lattice calculation results of the form factors for $B_{d,s}^*\to D, D_s(\pi, K)$ transitions are not yet available, we use their values evaluated in the BSW model [29,30]. Their values at zero-momentum transfer are listed below

$$A_0^{\bar{B}^*\to D}(0)=0.71,\quad A_1^{\bar{B}^*\to D}(0)=0.75,$$
$$A_2^{\bar{B}^*\to D}(0)=0.62,\quad V^{\bar{B}^*\to D}(0)=0.76,$$
$$A_0^{\bar{B}_s^*\to D_s}(0)=0.66,\quad A_1^{\bar{B}_s^*\to D_s}(0)=0.69,$$
$$A_2^{\bar{B}_s^*\to D_s}(0)=0.59,\quad V^{\bar{B}_s^*\to D_s}(0)=0.72,$$
$$A_0^{\bar{B}^*\to\pi}(0)=0.34,\quad A_1^{\bar{B}^*\to\pi}(0)=0.38,$$
$$A_2^{\bar{B}^*\to\pi}(0)=0.30,\quad V^{\bar{B}^*\to\pi}(0)=0.35,$$
$$A_0^{\bar{B}_s^*\to K}(0)=0.28,\quad A_1^{\bar{B}_s^*\to K}(0)=0.29,$$
$$A_2^{\bar{B}_s^*\to K}(0)=0.26,\quad V^{\bar{B}_s^*\to K}(0)=0.30. \tag{32}$$

The q^2 dependence of the form factors can be written as,

$$A_0(q^2)\simeq\frac{A_0(0)}{1-q^2/m_{B_q}^2(0^-)},\quad A_1(q^2)\simeq\frac{A_1(0)}{1-q^2/m_{B_q}^2(1^+)},$$

$$A_2(q^2)\simeq\frac{A_2(0)}{1-q^2/m_{B_q}^2(1^+)},\quad V(q^2)\simeq\frac{V(0)}{1-q^2/m_{B_q}^2(1^-)}, \tag{33}$$

Table 1 Values of pole masses in GeV

Current	$m(0^-)$	$m(0^+)$	$m(1^-)$	$m(1^+)$
$\bar{u}b$	5.27	5.99	5.32	5.71
$\bar{c}b$	6.30	6.80	6.34	6.73

where $m_{B_q}(0^\pm)$ and $m_{B_q}(1^\pm)$ are the pole masses whose values are presented in Table 1. In our analysis, we consider 10% uncertainty in the values of hadronic form factors at $q^2=0$.

3 Constraints on new couplings

In this analysis the new couplings are considered to be complex. Considering the contribution of only one coefficient at a time with all others set to zero, we perform the chi-square fitting for the individual complex couplings. The χ^2 is defined as

$$\chi^2=\sum_i\frac{(\mathcal{O}_i^{\text{th}}-\mathcal{O}_i^{\text{exp}})^2}{(\Delta\mathcal{O}_i)^2}, \tag{34}$$

where $\mathcal{O}_i^{\text{th}}$ represent the theoretical predictions of the observables, $\mathcal{O}_i^{\text{exp}}$ symbolize the measured central values of the observables and $(\Delta\mathcal{O}_i)^2=(\Delta\mathcal{O}_i^{\text{th}})^2+(\Delta\mathcal{O}_i^{\text{exp}})^2$ contain the 1σ errors from theory and experiment. We constrain the real and imaginary parts of new coefficients related to $b\to c\tau\bar{\nu}_\tau$ quark level transitions from the χ^2 fit of $R_{D^{(*)}}$, $R_{J/\psi}$ and $\text{Br}(B_c^+\to\tau^+\nu_\tau)$ observables and the couplings associated with $b\to u\tau\bar{\nu}_\tau$ processes are constrained from the fit of R_π^l, $\text{Br}(B_u^+\to\tau^+\nu)$ and $\text{Br}(B^0\to\pi^+\tau^-\bar{\nu})$ data. The updated values of all the observables used for fitting are taken from [20] and are listed in Table 2. The upper limit on the branching ratio of $B_c^+\to\tau^+\nu_\tau$ decay mode with the present world average of the B_c lifetime is [31]

$$\text{Br}(B_c^+\to\tau^+\nu_\tau)\lesssim 30\%. \tag{35}$$

We use the theoretical expressions of these observables and their SM predictions from [32] and have listed them in Table 2.

Table 2 Values of the observables used in the fitting

Observables	Experimental value	SM prediction
R_D	$0.340\pm0.027\pm0.013$	0.299 ± 0.003
R_{D^*}	$0.295\pm0.011\pm0.008$	0.258 ± 0.005
$R_{J/\psi}$	0.71 ± 0.251	0.289 ± 0.01
$\text{Br}(B_c\to\tau\nu)$	$<30\%$	$(3.6\pm0.14)\times10^{-2}$
R_π^l	0.699 ± 0.156	0.583 ± 0.055
$\text{Br}(B_u\to\tau\nu)$	$(1.09\pm0.24)\times10^{-4}$	$(8.48\pm0.5)\times10^{-5}$
$\text{Br}(B^0\to\pi^+\tau\nu)$	$<2.5\times10^{-4}$	$(9.40\pm0.75)\times10^{-5}$

Fig. 1 Constraints on individual new complex coefficients associated with $b \to c \tau \bar{\nu}_\tau$ processes from the χ^2 fit of $R_{D^{(*)}}$, $R_{J/\psi}$ and upper limit on $\mathrm{Br}(B_c^+ \to \tau^+ \nu_\tau)$. Here the red, blue and green colors stand for 1σ, 2σ and 3σ contours respectively. The black dots represent the best-fit values
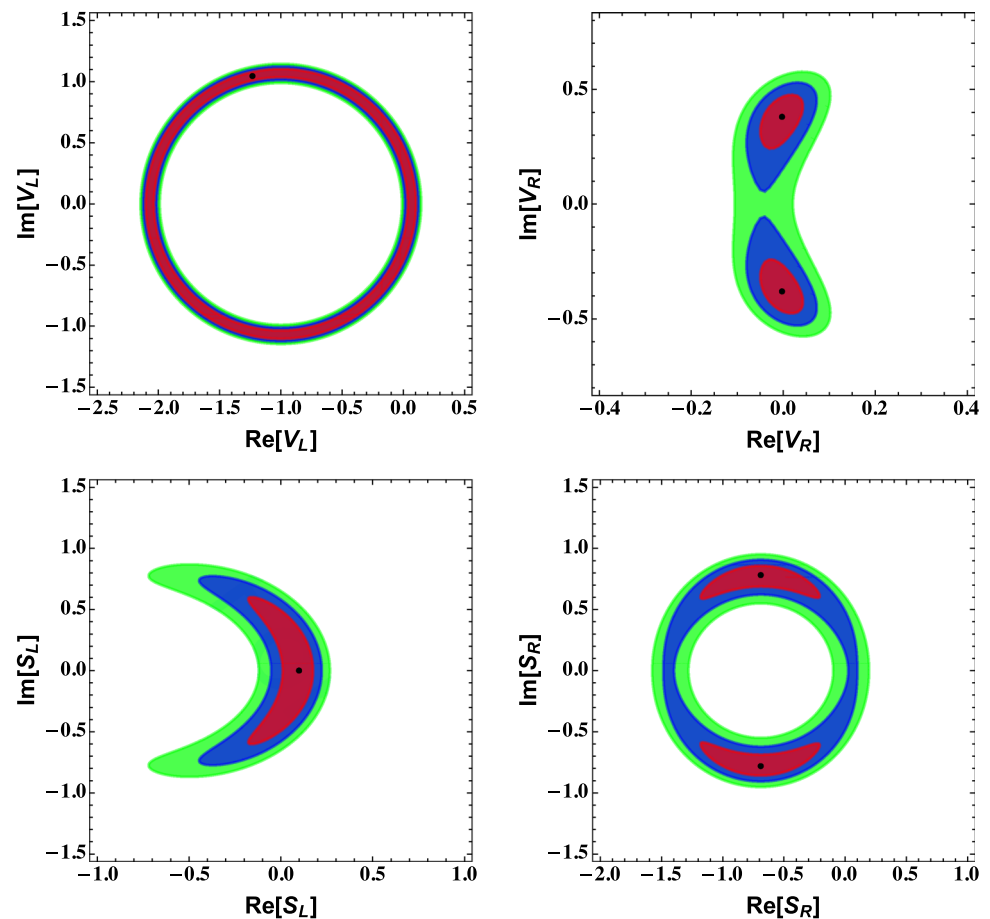
In Fig. 1, we present the constraints on V_L (top-left panel), V_R (top-right panel), S_L (bottom-left panel) and S_R (bottom-right panel) coefficients of $b \to c$ mediated decay modes and the corresponding plots for the coefficients of $b \to u$ are shown in Fig. 2. It should be noted that, the best-fit values are degenerate in the presence of V_L coupling (V_L, S_L and S_R couplings) for $b \to c$ ($b \to u$) processes and for each of these couplings, we have considered only benchmark values. The best-fit values and the corresponding 1σ ranges, which are obtained from the joint confidence regions of the real and imaginary planes of these new couplings, are presented in Table 3. The χ^2/d.o.f, as well as the pull $\simeq \sqrt{\chi^2_{\mathrm{SM}} - \chi^2_{\mathrm{best-fit}}}$, for all the coefficients are also listed in this Table. One can notice that, the Wilson coefficient corresponding to $b \to c$ scalar operators have χ^2/d.o.f > 1, which implies that the fit is not robust. However, the pull values of $V_{L,R}$ coefficients of $b \to c$ implicit that the measured data are consistent with our model in the presence of either V_L or V_R and can be a viable candidate for explaining the $b \to c \tau \bar{\nu}_\tau$ anomalies.

4 Effect of new coefficients on $B_{d,s}^* \to (D, D_s, \pi, K) \tau \bar{\nu}_\tau$ decay modes

After collecting all the theoretical expressions of required observables and getting knowledge on the allowed ranges of new parameters, we now proceed towards numerical analysis. The particles masses and the values of the CKM elements and the Fermi constant G_F are taken from PDG [20]. The values of the current quark masses used in this analysis are as $m_b = 4.2$ GeV, $m_c = 1.3$ GeV, and $m_u = 2.2$ MeV. The q^2 dependence of the form factors, required for numerical estimation are already discussed in section II. As the lifetimes of B^* mesons are not yet measured, we impose the fact that for these mesons the electromagnetic transitions $B^* \to B\gamma$ are the dominant ones, and hence $\Gamma_{\mathrm{tot}}(B^*) \simeq \Gamma(B^* \to B\gamma)$ and use the following results

$$\Gamma(B_d^* \to B_d\gamma) = 0.148 \pm 0.020 \text{ KeV} \quad [31]$$
$$\Gamma(B^{*+} \to B^+\gamma) = 0.468^{+0.073}_{-0.075} \text{ KeV} \quad [31]$$
$$\Gamma(B_s^* \to B_s\gamma) \simeq 0.07 \text{ KeV} \quad [32]. \quad (36)$$

Fig. 2 Constraints on individual new complex coefficients associated with $b \to u\tau\bar{\nu}_\tau$ processes from the χ^2 fit of R_π^l, $\mathrm{Br}(B_u^+ \to \tau^+\nu_\tau)$ and upper limit on $\mathrm{Br}(B^0 \to \pi^+\tau^-\bar{\nu}_\tau)$
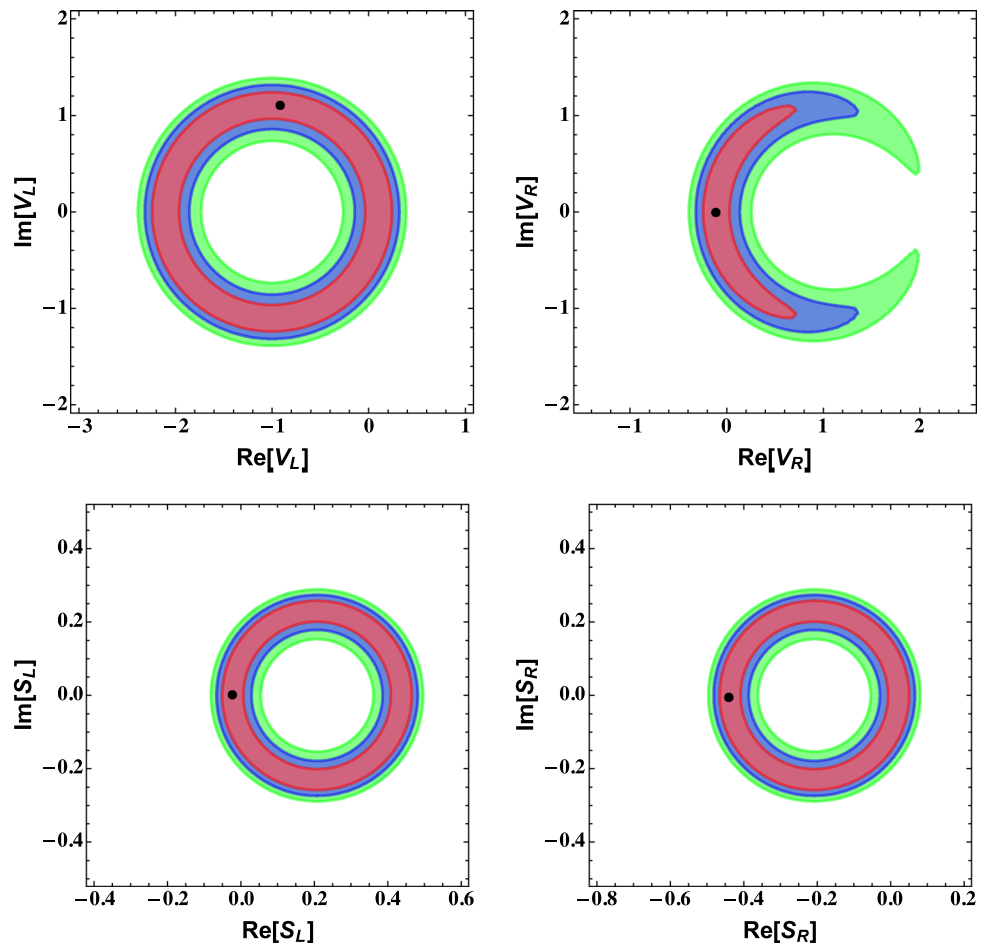
Table 3 Best-fit values and corresponding 1σ ranges (for one benchmark set only) of the new complex coefficients

Decay modes	New coefficients	Best-fit	1σ range	χ^2/d.o.f	Pull
$b \to c\tau\bar{\nu}_\tau$	$(\mathrm{Re}[V_L], \mathrm{Im}[V_L])$	$(-1.233, 1.045)$	$([-1.32, -1.075], [1.021, 1.067])$	1.151	2.982
	$(\mathrm{Re}[V_R], \mathrm{Im}[V_R])$	$(-0.0034, -0.3783)$	$([-0.030, 0.025], [-0.438, -0.31])$	1.145	2.984
	$(\mathrm{Re}[S_L], \mathrm{Im}[S_L])$	$(0.097, 0)$	$([0.041, 0.15], [-0.257, 0.257])$	4.213	1.663
	$(\mathrm{Re}[S_R], \mathrm{Im}[S_R])$	$(-0.695, -0.777)$	$([-0.93, -0.55], [-0.835, -0.72])$	2.175	2.616
$b \to u\tau\bar{\nu}_\tau$	$(\mathrm{Re}[V_L], \mathrm{Im}[V_L])$	$(-0.915, 1.108)$	$([-1.45, -0.65], [1.02, 1.19])$	0.131	1.160
	$(\mathrm{Re}[V_R], \mathrm{Im}[V_R])$	$(-0.116, 0)$	$([-0.205, -0.025], [-0.41, 0.41])$	0.066	1.215
	$(\mathrm{Re}[S_L], \mathrm{Im}[S_L])$	$(-0.024, 0)$	$([-0.042, -0.004], [-0.092, 0.092])$	0.093	1.192
	$(\mathrm{Re}[S_R], \mathrm{Im}[S_R])$	$(-0.439, 0.005)$	$([-0.457, -0.421], [-0.092, 0.092])$	0.093	1.192

From Eq. (36), it should be noted that $\Gamma_{\mathrm{tot}}(B^{*+} \simeq \frac{1}{3}\Gamma_{\mathrm{tot}}(B_d^*))$, so the branching fractions of $B^{*+} \to P\ell\nu_\ell$ processes are roughly one-third of $B_d^* \to P\ell\nu_\ell$. Hence, those results are not presented in this work. Furthermore, we assume that the new physics will couple only to third generation leptons, so the $B_{d,s}^* \to P\mu\nu_\mu$ processes will not be affected by the presence of new physics operators, and their standard model branching fractions are listed in Table 4, which are expected to be within the reach of LHC experiment.

The $\bar{B}_{d,s}^* \to (D, D_s)\tau^-\bar{\nu}_\tau$ processes proceed through $b \to c$ quark level transitions, so we use the constrained values of the new couplings obtained for $b \to c\tau\bar{\nu}_\tau$ in order to calculate the associated observables of these processes. Similarly we use the allowed parameter space obtained for $b \to u\tau\bar{\nu}_\tau$ process to compute the observables associated with $B_{d,s}^* \to (\pi, K)\tau^-\bar{\nu}_\tau$ decay process as they are mediated by $b \to u$ quark level transitions. In the following subsections, we discuss the effect of the presence of

Table 4 Branching fractions of $B_{d,s}^* \to P\mu\bar{\nu}_\mu$ processes in the Standard Model

Decay processes	SM branching fraction
$\mathrm{Br}(B^{*0} \to D^+\mu^-\bar{\nu}_\mu)$	$(9.318 \pm 1.901) \times 10^{-8}$
$\mathrm{Br}(B_s^* \to D_s^+\mu^-\bar{\nu}_\mu)$	$(1.709 \pm 0.349) \times 10^{-7}$
$\mathrm{Br}(B^{*0} \to \pi^+\mu^-\bar{\nu}_\mu)$	$(1.487 \pm 0.401) \times 10^{-9}$
$\mathrm{Br}(B_s^* \to K^+\mu^-\bar{\nu}_\mu)$	$(1.618 \pm 0.437) \times 10^{-9}$

one Wilson coefficient at a time on various observables of $B_{d,s}^* \to (D, D_s, \pi, K)\tau\nu_\tau$ decay modes.

4.1 Effect of V_L only

Here we consider the case, where the additional contribution to the SM Lagrangian arising only from V_L coefficient and all other new coefficients are set to zero i.e., $(S_L = S_R = V_R = 0)$. Using the best-fit values and 1σ allowed parameter space of V_L, obtained from the χ^2 fit of $R_{D^{(*)}}$, $R_{J/\psi}$, $\mathrm{Br}(B_c^+ \to \tau^+\nu)$ for $b \to c\tau\nu$ transitions (R_π^l, $\mathrm{Br}(B^0 \to \pi^+\tau^-\bar{\nu})$, $\mathrm{Br}(B_u^+ \to \tau^+\nu)$ for $b \to u\tau\nu$ transitions), we then calculate the differential decay rate, LNU observable, lepton spin asymmetry and forward–backward asymmetry of $B^{*0} \to D^+\tau\nu$ and $B_s^* \to D_s^+\tau\nu$ ($B^{*0} \to \pi^+\tau\nu$ and $B_s^* \to K^+\tau\nu$) decay processes. In the left panel of Fig. 3, we show the q^2 variation of decay rate (top) and R_D^* observable (bottom) of $B^{*0} \to D^+\tau\nu$ process and the corresponding plots for $B^{*0} \to \pi^+\tau\nu$ channel are presented in the right panel of this figure. Here the blue dashed lines correspond to the SM prediction and the cyan bands represent the 1σ uncertainty, arising due to the errors in CKM matrix elements, hadronic form factors and the lifetime of B^* meson. The solid black lines are obtained by using the best-fit values of the left handed vectorial new V_L coupling and the orange bands represent the 1σ allowed ranges, which includes the SM uncertainties as well as the uncertainties due to the new couplings. From the plots, one can notice significant deviation in the branching ratios and LNU observables from their corresponding SM predictions due to presence of additional V_L coefficient. To quantify these deviations, we define the pull metric at the observable level as

$$\mathrm{Pull}_i = \frac{\mathcal{O}_i^{\mathrm{NP}} - \mathcal{O}_i^{\mathrm{SM}}}{\sqrt{\Delta\mathcal{O}_i^{\mathrm{NP2}} + \Delta\mathcal{O}_i^{\mathrm{SM2}}}}, \tag{37}$$

where the index i runs over all observables, $\mathcal{O}_i^{\mathrm{SM}}$ and $\mathcal{O}_i^{\mathrm{NP}}$ denote the values of the observables in SM and NP scenarios and $\Delta\mathcal{O}_i^{\mathrm{SM}}$, $\Delta\mathcal{O}_i^{\mathrm{NP}}$ are the corresponding 1σ uncertainties. We thus, obtain $\mathrm{Pull}_{\mathrm{Br}\,(R_D^*)} = 0.530\,(4.0)$ for $B^* \to D^+\tau\nu$ process and $\mathrm{Pull}_{\mathrm{Br}\,(R_\pi^*)} = 0.399\,(1.239)$ for $B^* \to \pi\tau\nu$ process. The Pull value for R_D^* and R_π^* are found to be large as the SM uncertainties cancel out in these observ-

ables, thus providing significantly large pull value. The plots for $B_s^* \to D_s^+\tau\nu$ ($B_s^* \to K^+\tau\nu$) process follow the same form as $B^{*0} \to D^+\tau\nu$ ($B^{*0} \to \pi^+\tau\nu$), and hence, are not included in this article. The numerical values of these observables are presented in Table 5. Furthermore, no deviation has been observed in the forward–backward asymmetry and lepton-spin asymmetry observables from their SM results, so we don't provide the corresponding plots. The values of q^2 at which the forward–backward asymmetry vanishes are provided in Table 7.

4.2 Effect of V_R only

In this scenario, we explore the effect of only V_R coefficient on the decay rate and angular observables of $B^* \to (D^+, \pi^+)\tau\nu_\tau$ processes. Using the best-fit values and corresponding 1σ allowed ranges of V_R coefficients associated with $b \to (c, u)\tau\bar{\nu}_\tau$ transitions, we present the plots for the decay rate (left-top panel), R_D^* (left-middle) and forward–backward asymmetry (left-bottom panel) of $B^* \to D^+\tau\nu$ decay modes in Fig. 4. The corresponding plots for $B^* \to \pi^+\tau\nu$ process are depicted in the right panel of Fig. 4. Here the solid black lines are obtained by using the best-fit values of new V_R couplings and the gray bands by including 1σ uncertainties of all input values. Reasonable deviation in all the observables (except the lepton-spin asymmetry) from their SM results are found due to the presence of additional V_R coefficient, with Pull values $\mathrm{Pull}_{\mathrm{Br}/R_D^*/A_{\mathrm{FB}}} = 0.429/3.21/3.391$ for $B^* \to D^+\tau\nu$ process and $\mathrm{Pull}_{\mathrm{Br}/R_\pi^*/A_{\mathrm{FB}}} = 0.368/1.203/1.323$ for $B^* \to \pi\tau\nu$. In Table 5, we present the numerical values of decay rates and all these parameters. Due to the additional contribution from V_R coefficient, we notice deviation in the zero crossing of the forward–backward asymmetry towards high q^2 and the q^2 values of the zero crossing point are given in Table 7.

4.3 Effect of S_L only

In this subsection, we consider the contribution of S_L new coefficient by assuming that all other new Wilson coefficients have vanishing values. As seen from Figs. 1 and 2, the S_L parameters are severely constrained by the current data. Within the allowed parameter space for S_L coefficient presented in Table 3, we show the q^2 variation of lepton-spin asymmetry (top) and forward–backward asymmetry (bottom) of $B^* \to D^+\tau\bar{\nu}$ ($B^* \to \pi^+\tau\bar{\nu}$) process on the left panel (right panel) of Fig. 5. Here the plots obtained from the best-fit values (1σ range) of S_L coupling are represented by dashed black lines (red bands). The numerical values of these observables are given in Table 6. With the additional S_L contribution, the deviation in the branching ratios and LNU observables from their SM predictions are found to be
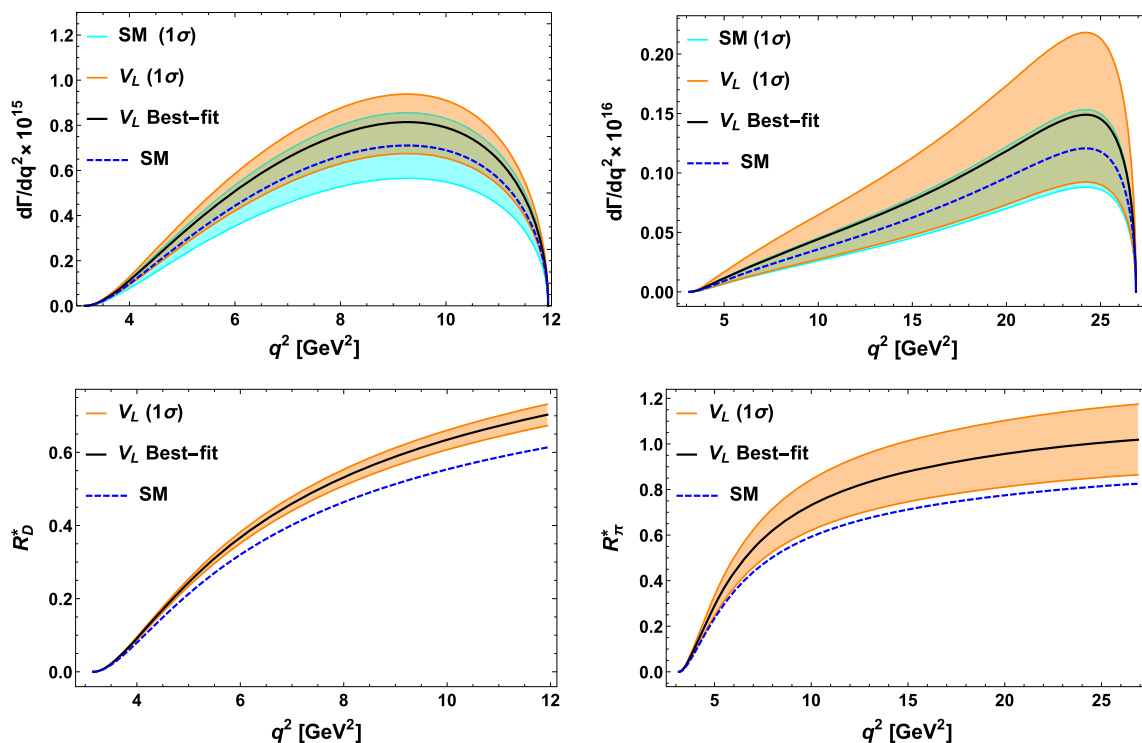
Fig. 3 The q^2 variation of differential decay rates and LNU observables of $\bar{B}_d^* \to D^+ \tau^- \bar{\nu}_\tau$ (left panel) and $\bar{B}_d^* \to \pi^+ \tau^+ \bar{\nu}_\tau$ (right panel) in presence of only V_L new coefficient. Here the blue dashed lines represent the standard model predictions. The black solid lines and the orange bands are obtained by using the best-fit values and corresponding 1σ range of V_L coefficient

Table 5 Predicted numerical values of differential decay rate, LNU observables, lepton spin asymmetry and forward–backward asymmetry of $\bar{B}_{d,(s)}^* \to D^+(D_s^+)\tau^-\bar{\nu}_\tau$ and $\bar{B}_{d(s)}^* \to \pi^+(K^+)\tau\bar{\nu}_\tau$ decay processes in the SM and in the presence of $V_{L,R}$ coefficients

Observables	SM Predictions	Values with V_L	Values with V_R
$\mathrm{Br}(B^{*0} \to D^+\tau^-\bar{\nu}_\tau)$	$(2.786 \pm 0.568) \times 10^{-8}$	$[2.646, 3.679] \times 10^{-8}$	$[2.444, 4.019] \times 10^{-8}$
R_D^*	0.299	$[0.328, 0.357]$	$[0.330, 0.358]$
A_λ^D	0.576	0.576	0.576
A_{FB}^D	-0.054	-0.054	$[-0.027, -0.004]$
$\mathrm{Br}(B_s^{*0} \to D_s^+\tau^-\bar{\nu}_\tau)$	$(5.074 \pm 1.035) \times 10^{-8}$	$[4.818, 6.701] \times 10^{-8}$	$[4.453, 7.320] \times 10^{-8}$
$R_{D_s}^*$	0.297	$[0.326, 0.354]$	$[0.327, 0.356]$
$A_\lambda^{D_s}$	0.573	0.573	0.573
A_{FB}^D	-0.053	-0.053	$[-0.025, -0.003]$
$\mathrm{Br}(B^{*0} \to \pi^+\tau^-\bar{\nu}_\tau)$	$(1.008 \pm 0.272) \times 10^{-9}$	$[0.771, 1.821] \times 10^{-9}$	$(0.767, 1.781) \times 10^{-9}$
R_π^*	0.678	$[0.710, 0.965]$	$[0.707, 0.943]$
A_λ^π	0.781	0.781	$[0.780, 0.781]$
A_{FB}^π	-0.209	-0.209	$[-0.198, -0.127]$
$\mathrm{Br}(B_s^{*0} \to K^+\tau^-\bar{\nu}_\tau)$	$(1.034 \pm 0.279) \times 10^{-9}$	$[0.791, 1.869] \times 10^{-9}$	$[0.787, 1.818] \times 10^{-9}$
R_K^*	0.639	$[0.670, 0.910]$	$[0.666, 0.885]$
A_λ^K	0.747	0.747	$[0.745, 0.746]$
A_{FB}^K	-0.207	-0.207	$[-0.196, -0.123]$

minimal. Though the lepton spin asymmetry and forward–backward asymmetry observables of $B^* \to D^+\tau\bar{\nu}$ channel provide slight deviation from their SM results, the deviation is negligible in the $B^* \to \pi^+\tau\bar{\nu}$ modes. The zero crossing point of the forward–backward asymmetry of $B^* \to D^+\tau\bar{\nu}$ process shifted sligtly towards the low q^2 region. The A_{FB}^P vanishing values of q^2 predicted from the best-fit values and 1σ range of new S_L coefficient are presented in Table 7.
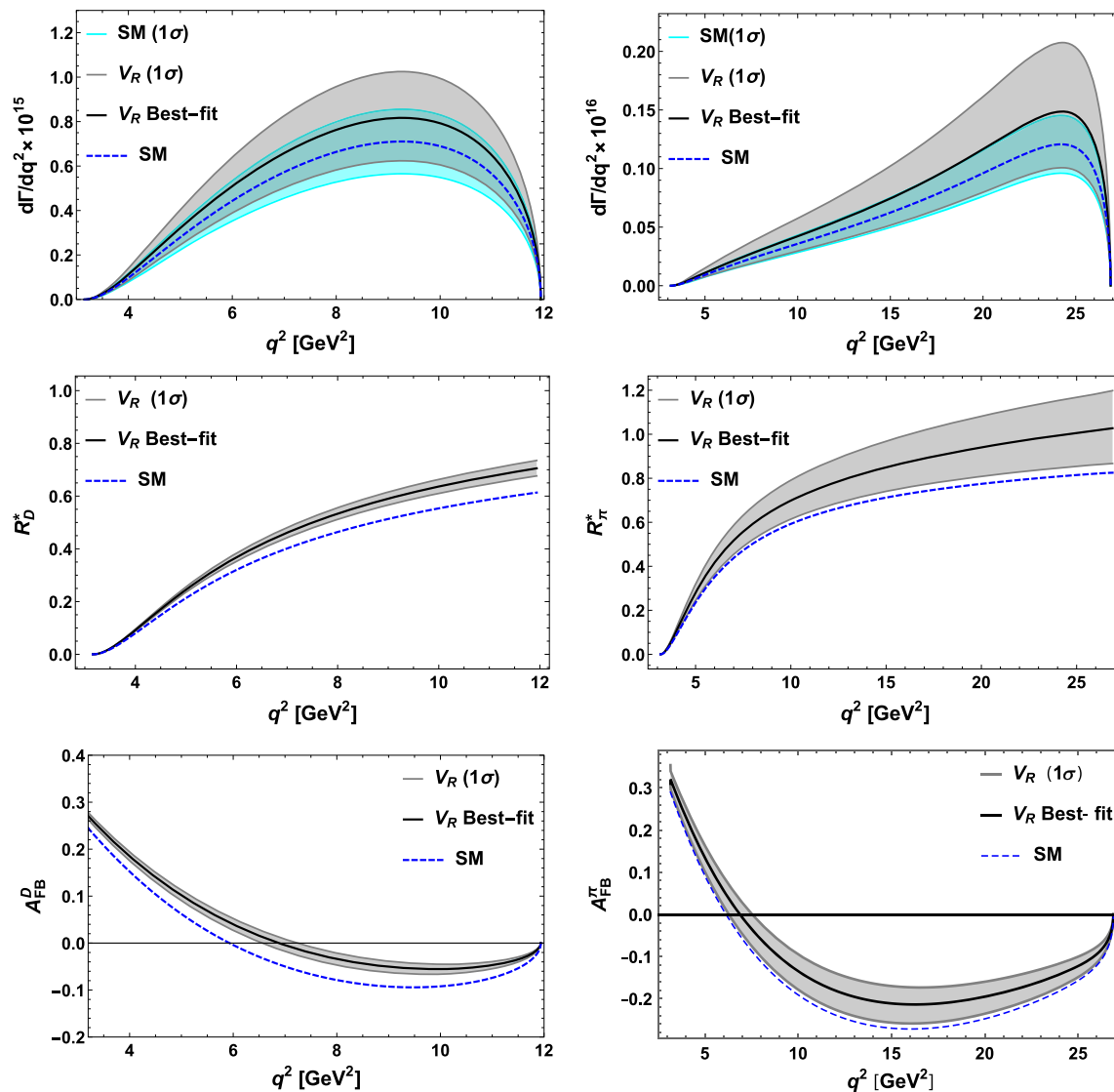
Fig. 4 The q^2 variation of differential decay rate, lepton nonuniversaity parameter and forward–backward asymmetry of $\bar{B}_d^* \to D^+ \tau^- \bar{\nu}$ (left panel) and $\bar{B}_d^* \to \pi^+ \tau \bar{\nu}$ (right panel) in presence of new V_R coef-ficient. The black solid lines and the gray bands are obtained by using the best-fit values and corresponding 1σ range of V_R coefficient

4.4 Effect of S_R only

Here we investigate the observables of $B^* \to (D^+, \pi^+)\tau\bar{\nu}$ decay modes by considering the presence of only additional S_R coefficient. Using the available experimental data on $b \to (u, c)\tau\bar{\nu}$ transitions, we fit the corresponding S_R coefficients, which is already discussed in section II. In the left panel of Fig. 6, we present the q^2 variation of decay rate (top), R_D^* (second from top), lepton spin asymmetry (third from top) and forward–backward asymmetry (bottom) of $B^* \to D^+ \tau\bar{\nu}$ and the corresponding plots for $B^* \to \pi^+ \tau\bar{\nu}$ are shown in the right panel. Here the black dashed lines (magenta bands) are obtained from the best-fit values (1σ range) of S_R coupling and other input parameters. In this case

also, the deviation in the lepton spin asymmetry and forward–backward asymmetry observables are comparatively large, whereas the deviations in the branching ratios and LNU observables are nominal. The numerical values are presented in Table 6. From Fig. 6, one can notice that the zero crossing point of the forward–backward asymmetry deviates significantly towards left (low q^2 region) and the corresponding q^2 values of the crossings are shown in Table 7.

5 Summary and conclusion

The rare decay modes of B mesons have been extensively studied both theoretically and experimentally in order to crit-
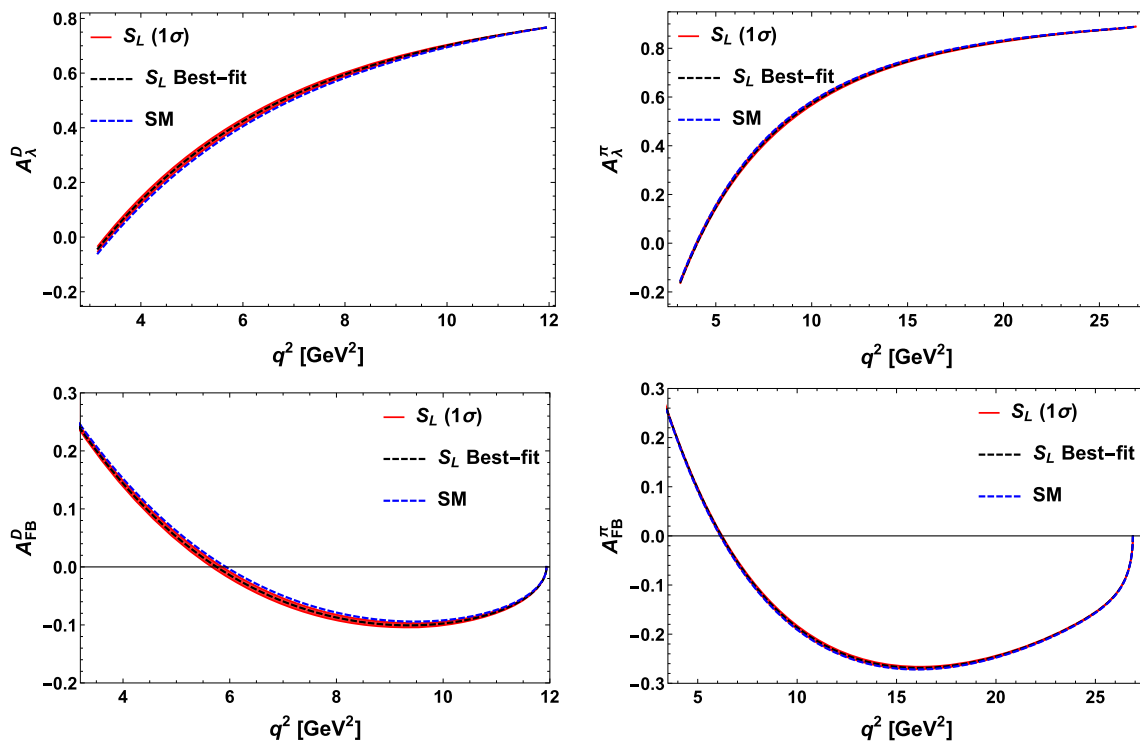
Fig. 5 The q^2 variation of lepton spin asymmetry and forward–backward asymmetry of $\bar{B}_d^* \to D^+ \tau^- \bar{\nu}_\tau$ (left panel) and $\bar{B}_d^* \to \pi^+ \tau^- \bar{\nu}_\tau$ (right panel) in presence of S_L coefficient only. The black dashed lines and the red bands are obtained by using the best-fit values and corresponding 1σ range of S_L coefficient

Table 6 Predicted numerical values of differential decay rate, LNU observables, lepton spin asymmetry and forward–backward asymmetry of $\bar{B}_{d(s)}^* \to D^+(D_s^+)\tau^-\bar{\nu}_\tau$ and $\bar{B}_{d,(s)}^* \to \pi^+(K^+)\tau\bar{\nu}_\tau$ decay processes in presence of $S_{L,R}$ coefficients

Observables	Values with S_L	Values with S_R
Br($B^{*0} \to D^+ \tau^- \bar{\nu}_\tau$)	$[2.193, 3.344] \times 10^{-8}$	$[2.180, 3.251] \times 10^{-8}$
R_D^*	$[0.296, 0.298]$	$[0.290, 0.294]$
A_λ^D	$[0.581, 0.594]$	$[0.604, 0.626]$
A_{FB}^D	$[-0.066, -0.058]$	$[-0.126, -0.096]$
Br($B_s^* \to D_s^+ \tau^- \bar{\nu}_\tau$)	$[3.993, 6.089] \times 10^{-8}$	$[3.968, 5.916] \times 10^{-8}$
$R_{D_s}^*$	$[0.293, 0.296]$	$[0.287, 0.292]$
$A_\lambda^{D_s}$	$[0.578, 0.591]$	$[0.601, 0.624]$
$A_{FB}^{D_s}$	$[-0.065, -0.056]$	$[-0.126, -0.095]$
Br($B^{*0} \to \pi^+ \tau^- \bar{\nu}_\tau$)	$[0.736, 1.285] \times 10^{-9}$	$[0.719, 1.250] \times 10^{-9}$
R_π^*	$[0.678, 0.680]$	$[0.662, 0.663]$
A_λ^π	$[0.774, 0.780]$	$[0.822, 0.823]$
A_{FB}^π	$[-0.208, -0.204]$	$[-0.254, -0.251]$
Br($B_s^* \to K^+ \tau^- \bar{\nu}_\tau$)	$[0.755, 1.320] \times 10^{-9}$	$[0.732, 1.273] \times 10^{-9}$
R_K^*	$[0.640, 0.642]$	$[0.619, 0.620]$
A_λ^K	$[0.738, 0.746]$	$[0.800, 0.802]$
A_{FB}^K	$[-0.207, -0.202]$	$[-0.260, -0.256]$

ically test the standard model prediction and to look for new physics beyond it. In this regard, the rare decay channels of the corresponding vector mesons i.e., the B^* decay modes are essential as they can provide complementary ways to go beyond the standard model. However, the weak decay channels of B^* vector mesons are not much explored experimen-

tally as they decay dominantly through electromagnetic process $B^* \to B\gamma$. Recently, with the advent of high luminosity LHCb experiment the sensitivity for the branching fractions of various rare decay modes is expected to reach the level $\sim \mathcal{O}(10^{-9})$. Thus, the LHCb would be an ideal platform to explore the rare decay modes of B^* mesons.
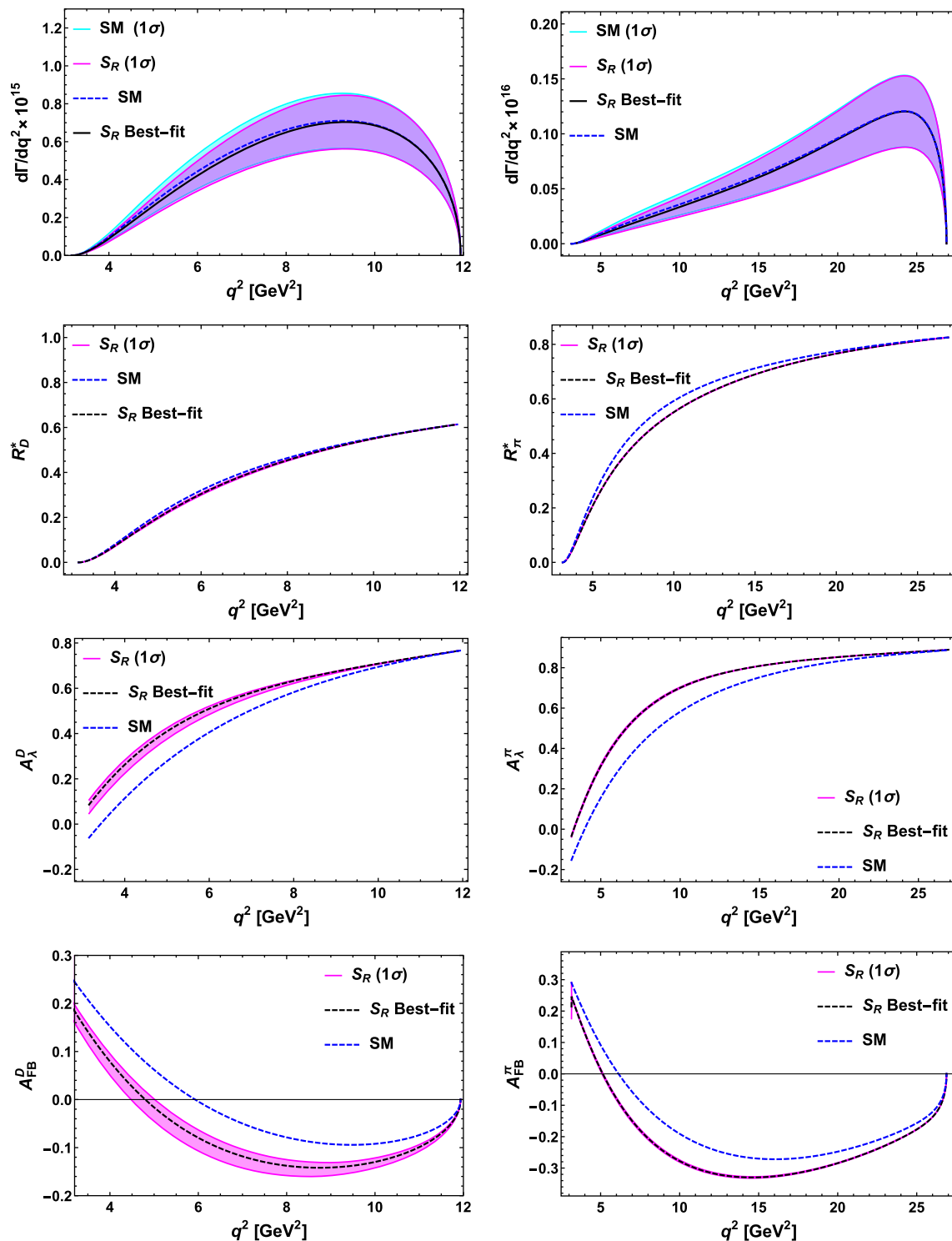
Fig. 6 The q^2 variation of differential decay rate, LNU observable, lepton spin asymmetry and forward–backward asymmetry of $\bar{B}^*_d \to D^+ \tau^- \bar{\nu}_\tau$ (left panel) and $\bar{B}^*_d \to \pi^+ \tau^- \bar{\nu}_\tau$ (right panel) in presence of S_R coefficient only. The black dashed lines and the magenta bands are obtained by using the best-fit values and corresponding 1σ range of S_R coefficient

In view of the recently observed anomalies $R_{D^{(*)}}$, $R_{J/\psi}$, R^l_π involving the charged current $b \to (c, u)l\nu$ transitions, we have performed a model independent analysis of the semilep-

tonic decay process of B^* vector meson decaying to a pseudoscalar meson P, where $P = D, D_s, \pi, K$, along with a charged lepton and corresponding antineutrino. We consid-

Table 7 The q^2 values (in GeV^2) of the zero crossing of forward–backward asymmetries of $B^*_{d,s} \to P\tau\bar{\nu}_\tau$ decay modes in the SM and in the presence of individual V_R, $S_{L,R}$ coefficients. The presence of additional V_L coefficient don't change the q^2 crossing values of the A^P_{FB}

Model	$B^*_d \to D\tau\bar{\nu}_\tau$	$B^*_d \to \pi\tau\bar{\nu}_\tau$	$B^*_s \to D_s\tau\bar{\nu}_\tau$	$B^*_s \to K\tau\bar{\nu}_\tau$
SM	5.93	6.13	5.96	6.26
V_R only (best-fit)	6.88	6.88	6.92	7.03
(1σ)	[6.56, 7.25]	[6.28, 7.54]	[6.59, 7.28]	[6.42, 7.70]
S_L only (best-fit)	5.75	6.19	5.78	6.33
(1σ)	[5.66, 5.85]	[6.14, 6.23]	[5.69, 5.88]	[6.28, 6.37]
S_R only (best-fit)	4.80	5.13	4.82	5.22
(1σ)	[4.48, 5.01]	[5.09, 5.17]	[4.49, 5.03]	[5.18, 5.26]

ered the generalized effective Lagrangian in the presence of vector and scalar type new physics operators. Considering only one new coefficient to be present at a time, and assuming the new couplings as complex, we constrained the new parameters associated with $b \to c\tau\bar{\nu}_\tau$ processes by performing χ^2 fit from $R_{D^{(*)}}$, $R_{J/\psi}$ parameters and the upper limit on $B^+_c \to \tau^+\nu_\tau$ branching fraction. The new couplings of $b \to u\tau\bar{\nu}_\tau$ processes are constrained by using experimental data on the branching ratios of $B_u \to \tau\nu_\tau$ and $B \to \pi\tau\nu_\tau$ and R^l_π parameter. Using the best-fit values and the corresponding 1σ ranges of new individual complex Wilson coefficients, we computed the branching ratios, forward–backward asymmetry, lepton spin asymmetry and lepton nonuniversality observables of $B^*_{d,(s)} \to D^+(D^+_s)\tau^-\bar{\nu}_\tau$ and $\bar{B}^*_{d,(s)} \to \pi^+(K^+)\tau\bar{\nu}_\tau$ decay processes. We have also shown the values of q^2 at which the forward–backward asymmetry vanishes. The branching fractions and LNU observables of these decay modes in the presence of additional V_L coefficient have significant deviations from their corresponding standard model predictions, whereas no deviations have been found in the lepton spin asymmetry and forward–backward asymmetry observables. Due to the additional contributions from V_R new coefficient, profound deviations have observed in the decay rates, lepton nonuniversality observable and the forward–backward asymmetry of both $\bar{B}^* \to (D,\pi)\tau\bar{\nu}_\tau$ processes. Due to the presence of V_R coupling, the zero crossing of forward–backward asymmetry has shifted towards high q^2 region for all decay modes. In the presence of S_L coefficient, none of the observables are affected and there is practically no deviation from SM results. Only the lepton-spin asymmetry and forward–backward asymmetry observables of $\bar{B}^* \to D\tau\bar{\nu}_\tau$ show slight deviation due to additional S_L coupling. On the other hand, in the presence of S_R coupling, the lepton spin asymmetry and the forward–backward asymmetry show reasonable deviations from their SM predictions and the decay rate lepton nonuniversality observables remain unchanged. The zero crossing of forward–backward asymmetry of all decay modes in the presence of S_R coefficient is found to be shifted towards low q^2 region. To conclude, we noticed significant deviations in some of the observables from their standard model predictions in pres-

ence of new couplings. The observation of these decay modes of vector B^* mesons at LHC experiment will definitely shed light on the nature of new physics.

References

1. J.P. Lees et al. (BaBar Collaboration), Phys. Rev. Lett. **109**, 101802 (2012)
2. J.P. Lees et al. (BaBar Collaboration), Phys. Rev. D **88**, 072012 (2013)
3. M. Huschle et al. (BaBar Collaboration), Phys. Rev. D **92**, 072014 (2015)
4. Y. Sato et al. (BaBar Collaboration), Phys. Rev. D **94**, 072007 (2016)
5. S. Hirose et al. (BaBar Collaboration), Phys. Rev. Lett. **118**, 211801 (2017)
6. R. Abdesselam et al. (Belle Collaboration), arXiv:1904.08794 [hep-ex]
7. R. Aaij et al. (LHCb Collaboration), Phys. Rev. Lett. **115**, 111803 (2015) [Erratum: Phys. Rev. Lett. **115**, 159901 (2015)]
8. R. Aaij et al. (LHCb Collaboration), Phys. Rev. Lett. **120**, 171802 (2018)
9. R. Aaij et al. (LHCb Collaboration), Phys. Rev. D **97**, 072013 (2018)
10. Heavy Flavour Averaging Group, https://hflav-eos.web.cern.ch/hflav-eos/semi/spring19/html/RDsDsstar/RDRDs.html
11. R. Aaij et al. (LHCb Collaboration), Phys. Rev. Lett. **120**, 121801 (2018)
12. W.-F. Wang, Y.-Y. Fan, Z.-J. Xiao, Chin. Phys. C **37**, 093102 (2013)
13. M.A. Ivanov, J.G. Korner, P. Santorelli, Phys. Rev. D **71**, 094006 (2005) [Erratum: Phys. Rev. D **75**, 019901 (2007)]
14. R. Aaij et al. (LHCb Collaboration), Phys. Rev. Lett. **113**, 151601 (2014)

15. R. Aaij et al. (LHCb Collaboration), JHEP **08**, 055 (2017)
16. C. Bobeth, G. Hiller, G. Piranishvili, JHEP **12**, 040 (2007)
17. B. Capdevila, A. Crivellin, S. Descotes-Genon, J. Matias, J. Virto, JHEP **01**, 093 (2018)
18. T. Humair (for the LHCb Collaboration), "Lepton Flavor Universality tests with heavy flavour decays at LHCb," talk given at Moriond, March 22 2019. See also R. Aaij et al. [LHCb Collaboration], "Search for lepton-universality violation in $B^+ \rightarrow K^+ l^+ l^-$ decays," CERN-EP-2019-043, 22 March (2019)
19. M. Prim (for the Belle Collaboration), "Search for $B \rightarrow l \nu \gamma$ and $B \rightarrow \mu \nu_\mu$ and Test of Lepton Universality with R_{K^*} at Belle," talk given at Moriond, March 22 (2019)
20. M. Tanabashi et al., (Particle Data Group), Phys. Rev. D **98**, 030001 (2018)
21. Q. Chang, J. Zhu, X.-L. Wang, J.-F. Sun, Y.-L. Yang, Nucl. Phys. B **909**, 921 (2016)
22. B. Grinstein, J.M. Camalich, Phys. Rev. Lett. **116**, 141801 (2016)
23. S. Sahoo, R. Mohanta, J. Phys. G **44**, 035001 (2017)
24. D. Kumar, J. Saini, S. Gangal, S.B. Das, Phys. Rev. D **97**, 035007 (2018)
25. S. Kumbhakar, J. Saini, arXiv:1807.04055
26. Q. Chang, J. Zhu, N. Wang, R.-M. Wang, Adv. High Energy Phys. **2018**, 7231354 (2018)
27. J. Zhang, Y. Zhang, Q. Zeng, Ruirui Sun, Euro Phys. J. C **79**, 164 (2019)
28. M. Tanaka, R. Watanabe, Phys. Rev. D **87**, 034028 (2013)
29. M. Wirbel, B. Stech, M. Bauer, Z. Phys. C **29**, 637 (1985)
30. M. Bauer, B. Stech, M. Wirbel, Z. Phys. C **34**, 103 (1987)
31. A.G. Akeroyd, C.-H. Chen, Phys. Rev. D **96**, 075011 (2017). arXiv:1708.04072
32. A. Ray, S. Sahoo, R. Mohanta, Phys. Rev. D **99**, 015015 (2019)
33. Chi-Yee Cheung, Chien-Wen Hwang, JHEP **04**, 177 (2014). arXiv:1401.3917
34. A. Khodjamirian, T. Mannel, Alexey A. Petrov, JHEP **11**, 142 (2015). arXiv:1509.07123